J Mater Sci: Mater Med (2008) 19:3227–3234
DOI 10.1007/s10856-008-3425-2

In vitro degradation of poly-L-D-lactic acid (PLDLA) pellets and powder used as synthetic alloplasts for bone grafting

M. E. R. Coimbra · C. N. Elias · P. G. Coelho

Received: 17 October 2007 / Accepted: 5 March 2008 / Published online: 3 May 2008

Abstract The objective of this study was to evaluate the in vitro degradation of pellet and powder forms of a poly-L-D-lactic acid material used to produce plates and screws for orthopedic, oral, and maxillofacial applications. *Materials and methods* In order to produce the powder form the as-received pellets were milled in a cryogenic chamber. Particles size distribution (PSD) histograms were developed for both forms. The materials were then characterized by Scanning Electron Microscopy (SEM), Differential Scanning Calorimetry (DSC), and Thermogravimetric Analysis (TGA) before and after immersion in simulated body fluid for 30, 60, and 90 days. *Results* SEM showed that for both forms material degradation started after 30 days of immersion in SBF and evolved until 90 days. Degradation started at the amorphous zones of the polymer and exposed of deeper crystalline layers. The pellet and powder samples PSD showed polydispersed patterns with mean diameters of 673.98 μm and 259.55 μm. Thermal onset degradation temperatures were 365.64°C and 360.30°C, and of 363.49°C and 359.83°C before immersion and after 90 days in SBF for the pellet and powder forms, respectively. The Tg's of the pellets and the powder were approximately 61.5°C and 66°C, and their respective endothermic peaks were observed at approximately 125°C and 120°C. The specific heat (c) was approximately 8.5 J/g and 6.2 J/g for the pellet and powder material, respectively. *Conclusion* According to the results obtained, cryogenic milling resulted in particle plastic deformation, and alterations in glass transition temperature, melting temperature, and specific heat of the material.

M. E. R. Coimbra (✉) · C. N. Elias
Department of Materials Science, Instituto Militar de Engenharia (IME), Praça General Tibúrcio, 80, Rio de Janeiro RJ 22290-270, Brazil
e-mail: maria.coimbra@gmail.com

M. E. R. Coimbra · P. G. Coelho
Department of Biomaterial and Biomimetics, College of Dentistry, New York University, 345 East 24th Street, Room 804S, New York, NY 10100, USA

1 Introduction

Bone grafting is a surgical technique used to repair large skeletal defects. For instance, when trauma or a degenerative disease causes the loss of significant portions of bone, the remaining tissue may have difficulty restoring its form and function [1]. In extensive bone tissue loss cases, it is recommended that scaffold is placed at the defect site in order to allow the adjacent bone to bridge the gap created by the defect [2]. These bone defects can be filled with a customized scaffold or with bone grafting materials typically available in powder form.

A common grafting material is the autogenous trabecular bone taken from a secondary surgical site [3]. Other types of grafting materials include allografts such as demineralized bone matrix particles [4], deproteinized cancellous chips [4], or synthetic alloplasts such as calcium sulfate pellets and porous calcium phosphate materials [4]. Although autogenous bone grafting represents the standard clinical practice [3–5], synthetic bone grafting materials have increased in popularity over the last 10 years. This increase in the interest concerning synthetic materials has been due to the intrinsic problems associated with the use of autogenous bone grafts. Limitations such as supply, donor site pain and potential post-surgical infection, and unpredictable healing kinetics have

stimulated the development of synthetic materials/matrices engineered specifically for bone replacement applications [3–5].

Alternative to metallic devices, biodegradable polymers are of interest for bone fracture fixation, bone grafting fixation, and reconstruction of the anterior cruciate ligament [6]. The property that makes biodegradable fracture fixation devices more attractive than metallic ones is that no second surgical intervention for device removal procedure is needed after tissue has healed [7].

As scaffolds, biodegradable polymers offer a number of advantages over other materials such as bioceramics. These biodegradable polymers have some key advantages, such as: the tailor-ability of their mechanical properties and degradation kinetics to suit various applications. Synthetic polymers can be fabricated into various shapes with desired pore morphologic features conducive to tissue integration [8]. Furthermore, polymers can be designed with chemical functional groups that can induce tissue in-growth [8].

The majority of synthetic polymeric replacements under active investigation are based on biodegradable polymers [9]. The most commonly utilized biodegradable polymers are the aliphatic polyesters, such as polylactic acid (PLA), polycaprolcatone (PCL), polyethylene oxide (PEO), poly(3-hydroxybutyrate) (PHB), and polyglycolic acid (PGA) [10].

Two homopolymers, PLA D-lactide and L-lactide, form the synthetic blend PLA DL-lactide. The second one is a semi crystalline polymer. Poly(DL)lactide (DLPLA) is an amorphous polymer having a random distribution of both isomeric forms of lactic acid and thereby is unable to arrange into a crystalline organized structure during solidification processing [11]. The degradation kinetics of LPLA is much slower than that of DLPLA. Full degradation of LPLA has been reported to be greater than 2 years in vitro and in vivo studies [12]. Copolymers of L-lactide with glycolide or with DL-lactide have been prepared to disrupt the L-lactide crystallinity and thus accelerating the degradation process [13].

The biodegradation process of bioabsorbable polymers starts by water diffusion inside the material, hydrolysis breaking the polymeric chains, which results in less resistance and decrease in the polymer structural and chemical stability. Synergistic to hydrolysis, lisossomic enzymes and fibrous encapsulation also take part in the bioabsorbable polymers degradation process [14]. The in vivo and in vitro degradation produce lactic acid and glycolic acid monomers, which are metabolized into carbon dioxide and water, and are subsequently eliminated by lungs and kidney through the tricarboxylic acid cycle [7]. The process has higher kinetics at the amorphous zones of the polymer, increasing the fraction of crystalline zones, more resistant to the degradation process [11].

The cryogenic milling technique (brittle fracture technique) is a process carried out at low temperatures [15] either by using dry ice-acetone (−78°C) or liquid nitrogen (−196°C) [16]. The milling at lower temperatures leads to smaller particle sizes [17]. Liquid nitrogen provides the refrigeration required to pre-cool the samples and to maintain the low temperature by absorbing the heat generated during the milling process [15]. The principles of this technique are: hardness increase of the material to be grinded, insertion of failures in the structure, and reduction of the samples to small pieces by the use of very smooth brittle force [18]. It can be used for different types of samples such as thermoplastic, elastic, or fibrous materials that cannot yet be ground as efficiently as brittle materials [19].

PLDLA is commonly used as plate and screw for orthopedic intervention, or as scaffold for filling large defects, but its use as a powder for bone regeneration has not been thoroughly investigated to date. The purpose of this study was to characterize/evaluate the in vitro degradation of poly-L-D-lactic acid pellets and powder forms for bone grafting applications.

2 Materials and methods

Pellet-shaped samples of poly-L-D-lactic acid (PLDLA 70/30-Purac®, Gorinchen, The Netherlands) used in the fabrication of bioabsorbable plates and screws were utilized. Part of the material was transformed into powder by cryogenic milling using an oscillating magnetic bar [20] (Freezer Mill 6800) in order to allow a comparison between the in vitro behavior of pellet and powder forms (to simulate maxillofacial type particulate grafting applications) (Fig. 1). The system was pre-cooled for 5 minutes using liquid nitrogen (−196°C) and then three cycles of four minutes were performed to reduce the particle size of the PLDLA pellets. Eight groups were divided as follows: G1—pellets, as-received; G2—pellets, 30 days in SBF (simulated body fluid) [21]; G3—pellets, 60 days in SBF; G4—pellets, 90 days in SBF; G5—powder, as received; G6—powder, 30 days in SBF; G7—powder, 60 days in SBF; G8—powder, 90 days in SBF.

For the different groups' degradations kinetics assessment, the samples were placed in glass containers containing SBF solution at 37°C. One gram of each material was submersed in a 5:1 solution/material volume ratio in separate containers according to their degradation times. After 30, 60, and 90 days in solution, the samples were thoroughly washed with distilled water for 10 minutes and paper dried.

For Scanning Electron Microscopy (SEM) analysis, the material was coated three times with gold (Balzers Union

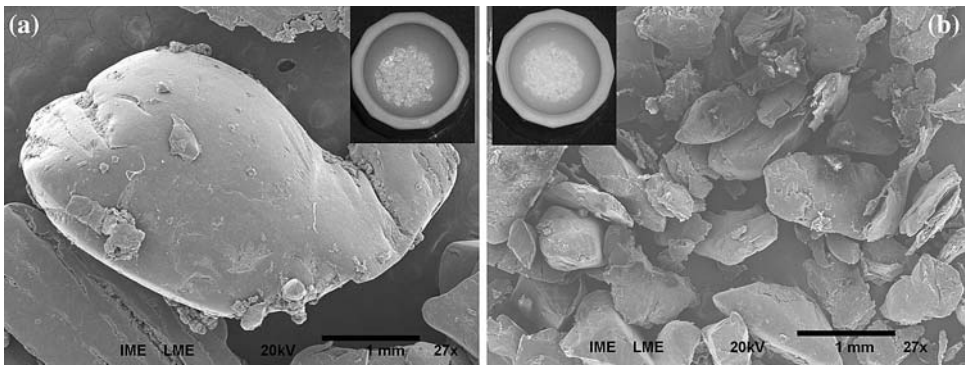

Fig. 1 PLDLA (70/30) pellets (**a**) Before milling SEM micrograph and the material as received (detail), (**b**) After milling, SEM micrograph and as the material looked like after the milling process (detail)

Sputtering Device, Principality of Liechtenstein). The analysis was made using a JEOL JSM 5800 LV microscope (Tokyo, Japan) with an acceleration voltage of 20 kV. The samples were analyzed with magnifications ranging from 27 to 2,000 ×. Surface texture and morphology evaluation were recorded before immersion in SBF solution, and at 30, 60, and 90 days in solution.

For the particle size distribution a small amount of pellets and powder granules were spread on a black cloth. The samples were observed under an optical microscope (Zeiss Stemi 2000-C, Germany) and 15 images of samples' different fields were obtained by means of a digital camera (PixeLink, PL-A662, Canada). A specific routine was developed under the KS400 software (Carl Zeiss Vision, Germany). The routine followed the typical sequence of image acquisition, pre-processing, segmentation, post-processing and measurements reported elsewhere [22]. Particles size histograms and cumulative distributions were generated for the pellets and powder. The cumulative distribution curves revealing the samples' particle size at 10, 50 and 90% of the total volume were determined.

Thermal analysis data was measured by Thermogravimetry (TGA) ($n = 5$) (SHIMADZU TGA-50, Kyoto, Japan) and Differential Scanning Calorimetry (DSC) ($n = 5$) (SHIMADZU DSC 50, Kyoto, Japan). All measurements were performed under nitrogen with a rate flow of 20 ml/min.

The thermal degradation behavior of the pellet and powder forms was evaluated before and after 90 days of degradation (pellets—G1 and G4 groups; powder—G5 and G8 groups). The thermal behavior was recorded by heating the samples from room temperature to 500°C at a rate of 20°C/min.

Differential Scanning Calorimetry (DSC) was utilized for glass transition temperature (T_g), melting temperature (T_m) and specific heat determination. Approximately 5 mg of material was placed in an aluminum container. The equipment was calibrated with high purity (99.9%) indium. The initial temperature for analysis was room temperature, which was increased at a rate of 10°C/min until reaching 320°C. Glass transition temperature (T_g) and melting point (T_m) determination from the DSC data were obtained by the curve's first derivative partial minimums, and the specific heat determination was obtained by calculating the area under the curve of the T_m peak and dividing it by the material's mass.

Thermal analysis statistical evaluation was performed by ANOVA and multiple comparisons were performed by the Tukey post-hoc test. The level of significance was set to 95%.

3 Results

3.1 Scanning Electron Microscopy (SEM)

A representative scanning electron micrograph of the as-received pellet shape PLDLA material (G1) is shown in Fig. 2a. The particles in Fig. 2a presented regions of smooth and rough granular morphology. After 30 days in SBF (G2), the pellets presented an increase in surface irregularities, and regions of fibrous configuration, confirming initial material loss to the medium (Fig. 2b). Figure 2c is representative of the pellets after 60 days in SBF (G3). The granular part of the material presented rounded edges compared to the pellet's morphology without degradation (Fig. 2a). The polymer's smooth portion presented surface delaminations (Fig. 2c). The morphology of the pellet form after 90 in SBF (G4) is shown in Fig. 2d. Higher degradation degrees were observed for the G4 group compared to the other groups. At originally smooth surfaces, more delaminations and irregularities indicated a progression in material degradation. In addition, blister-like features indicated that deeper layers have been exposed and started to degrade. The portion with granular morphology maintained the same pattern observed for pellets at 30 and 60 days in SBF (G2) (Fig. 2b and c).

The milling to powder form resulted in material's surface plastic deformation (G5) (Fig. 3a). However, the material maintained the same partially smooth morphology

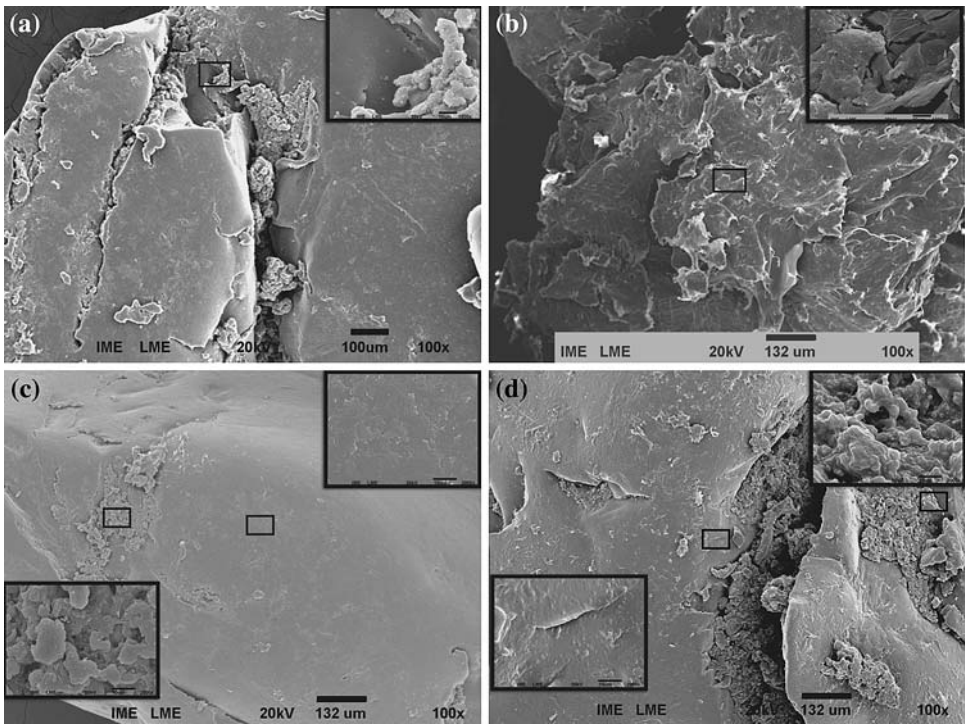

Fig. 2 PLDLA before milling micrographs: (**a**) As received (G1) (100×) (detail 1,500×); (**b**) After 30 days in SBF solution (G2) (100×) (detail 1,500×); (**c**) After 60 days in SBF solution (G3) (100×) (detail 2,000×); (**d**) After 90 days in SBF solution (G4) (100×) (detail 2,000×)

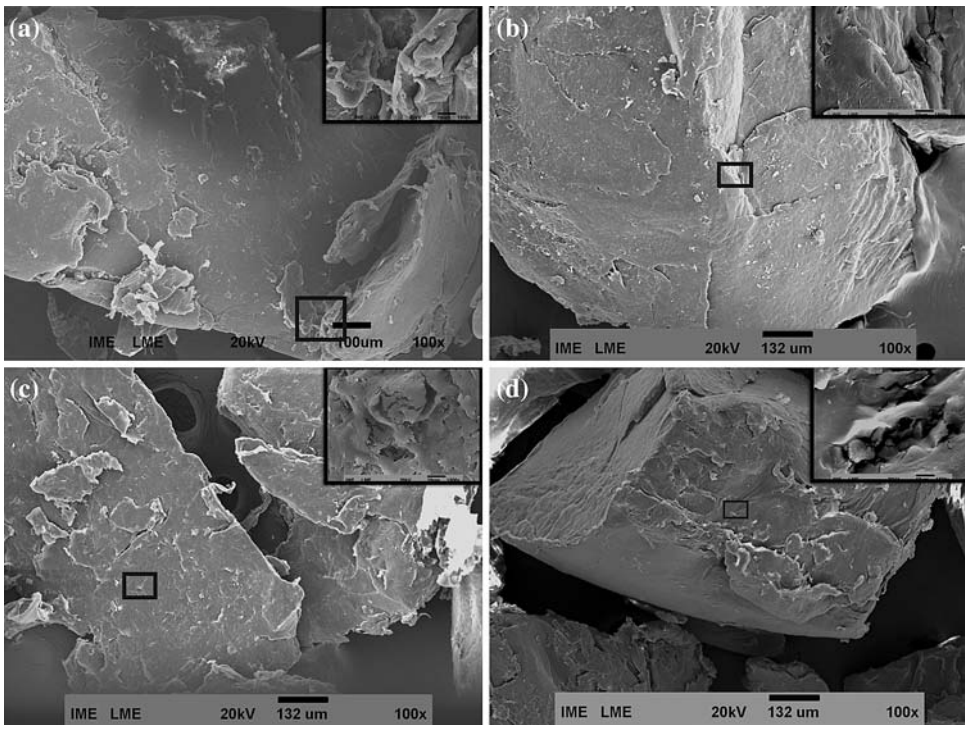

Fig. 3 PLDLA after milling micrographs: (**a**) As received (G5) (100×) (detail 1,500×); (**b**) After 30 days in SBF solution (G6) (100×) (detail 1,500×); (**c**) After 60 days in SBF solution (G7) (100×) (detail 1,500×); (**d**) After 90 days in SBF solution (G8) (100×) (detail 1,500×)

with rough granular regions surface pattern observed in the as-received pellet form (Fig. 2a). The powder sample (G6) showed smooth surfaces and delamination regions indicating material degradation after 30 days in SBF (Fig. 3b). Figure 3c is representative of the powder material morphology after 60 days in SBF (G7). The surface was more irregular and presented higher amounts of cracks, indicating that degradation process was more advanced compared to the after 30 days powder in SBF (Fig. 3a, b). Higher magnifications revealed voids indicating increased material loss. The powder sample that remained 90 days (G8) in SBF showed different patterns of degradation, where its

surface presented a globular appearance (Fig. 3d). Higher magnification showed fibrous connections within particle irregularities (Fig. 3d)

3.2 Particle size distribution

The particle size distribution showed a polydispersed pattern for both pellet and powder forms (Figs. 4a and 5a). The mean diameters were 673.98 μm and 259.55 μm for the pellet and powder forms, respectively. The cumulative distribution curves (Fig. 4b and 5b) revealing the samples' particle size at 10, 50 and 90% of the total volume are shown in Table 1.

3.3 Thermogravimetric Analysis (TGA)

The results of the TGA are shown in Fig. 6 and Table 2. The thermal degradation onset temperature for the pellets samples were 365.64°C and 360.30°C for the as-received (G1) and after 90 days degradation groups (G4), respectively. The powder form presented thermal degradation onset temperatures of 363.49°C and 359.83°C for the as received (G5) and after 90 days degradation groups (G8). No significant differences were observed between pellet and powder samples ($P > 0.05$).

Table 1 Mean particle diameters at different volumes

Amounts of samples vol (%)	Diameter values obtained	
	Pellet (μm)	Powder (μm)
D 10	500	19.05
D 50	676.32	290.48
D 90	847.37	461.90

3.4 Differential Scanning Calorimetry (DSC)

The results of DSC are presented in Fig. 7 and Table 3. The T_g's of the pellets and powder were approximately 61.5°C and 64.6°C, respectively. The endothermic peaks at

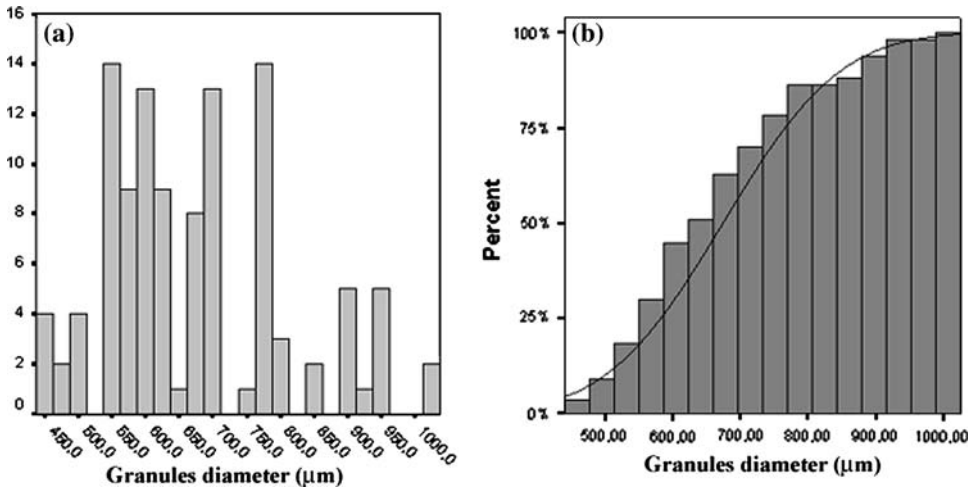

Fig. 4 Particle Size Distribution of PLDLA before milling

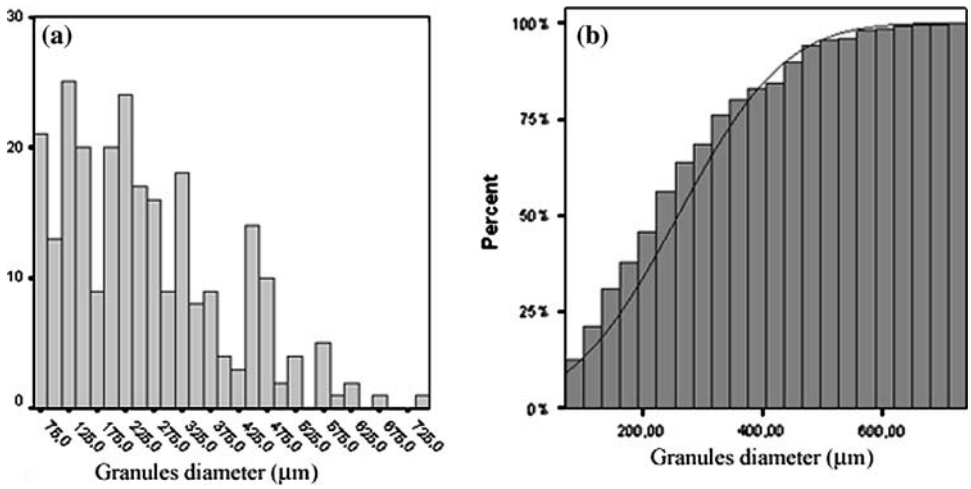

Fig. 5 Particle Size Distribution of PLDLA after milling

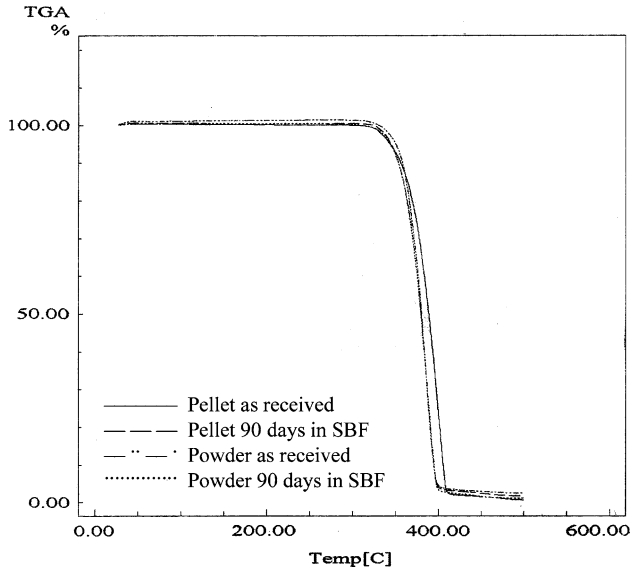

Fig. 6 TGA thermograms of PLDLA before and after milling as received and after 90 days in SBF solution

Table 2 TGA results

Groups		Onset (°C)/SD	Mass loss (mg/%)/SD
Pellet	As received	365.6/4.4[a]	98.9/0.7[a]
	90 days of degradation	360.3/3.9[a]	98.6/0.8[a]
Powder	As received	363.5/4.4[a]	98.5/0.2[a]
	90 days of degradation	359.8/2.2[a]	98.6/0.2[a]

[a] No significance ($P > 0.05$)

approximately 125°C and 120°C were related to the melting points (T_m) of PLDLA pellet and powder forms, respectively. In general, powder T_g's were higher than pellets, and powder T_m's lower than pellets (Table 3). We observed that the material's specific heat decreased from approximately 8.5 J/g to approximately 6.2 J/g after the milling process (Table 3). Significant differences were observed between pellet and powder samples ($P < 0.05$) for T_g, T_m, and specific heat (Table 3).

Table 3 DSC results

Groups		Peak 1st Derivate T_g (°C) /SD	Peak T_m (°C)/SD	Specific Heat (J/g)/SD
Pellet				
As-received	G1	60.6/1.1[a]	124.7/0.8[a]	8.8[a]
30 days	G2	61.9/0.2[a]	124.0/1.0[a]	8.5[a]
60 days	G3	61.8/1.0[a]	124.5/0.7[a]	8.4[a]
90 days	G4	61.5/0.8[a]	124.7/1.0[a]	8.2[a]
Powder				
As-received	G5	60.6/1.0[a]	120.3/0.5[b]	6.1[b]
30 days	G6	65.9/0.4[b]	119.9/0.3[b]	6.7[b]
60 days	G7	66.2/0.4[b]	119.8/0.3[b]	5.8[b]
90 days	G8	66.0/0.5[b]	119.9/0.2[b]	6.2[b]

[a] No significance ($P > 0.05$)

[b] Significance ($P < 0.05$)

4 Discussion

Significant effort has been devoted in an attempt to improve biomaterials used for grating applications. Studies with biodegradable polymers have concentrated in tailoring their mechanical properties and degradation kinetics to suit various applications. In addition, specific engineering of tissue conductive and/or inductive chemical functional groups is highly desirable [8].

The results obtained in our study showed that the degradation of both pellets and powder forms started after 30 days of immersion in SBF solution, and that process continued until the 90 days of degradation. In general, there was an indication that the degradation started at the amorphous zone of the polymer, and resulted in the

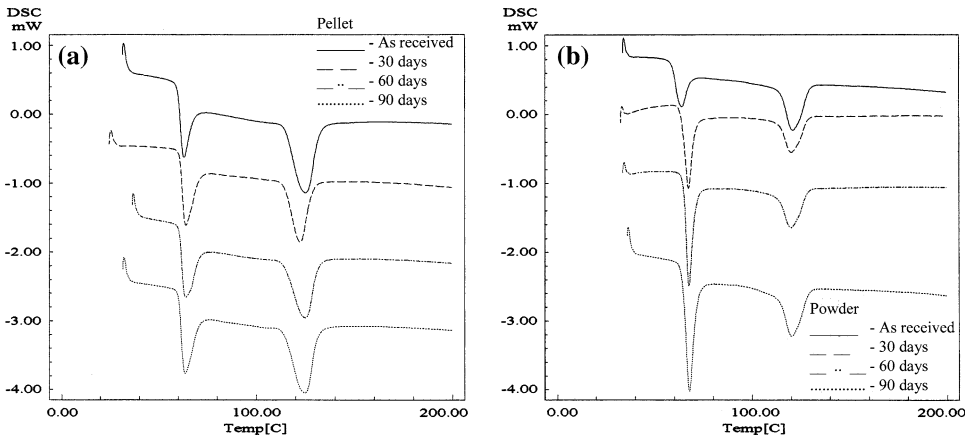

Fig. 7 DSC thermograms of PLDLA: (**a**) Before milling and (**b**) After milling

exposure of a deeper crystalline layer (Figs. 2 and 3), as previously depicted by Landes et al. [23] and Ribeiro et al. [24].

Specific to the in vitro and in vivo behavior of biodegradable polymers behavior, Landes et al. [23] compared degradation rates of poly(70L-lactide-co-30DL-lactide) (P(L/DL)LA) and poly(85L-lactide-co-15-glycolide) (PLGA) in patients (maxillofacial region) and in vitro. In human subjects, P(L/DL)LA's initial average molecular weight of 45,000 decreased to 25,000 (3 months), to 21,000 (6 months), and to 8000 (18 months). PLGA's average molecular weight decreased from 44,600 to 22,000 after 3 months in patients and in vitro, and to 11,000 in patients and 1300 in vitro at 6 months. In-patients and in vitro glass-transition temperatures decreased from ~60°C to 50°C over 18 months. Both copolymers decomposed reliably in patients: 85:15 PLGA within 12 months and 70:30 P(L/DL)LA within 24 months on average. They [23] also observed that the in vitro rates were significantly faster.

The degradation kinetics observed in the present study (not complete by 90 days) was slower than the one observed by Vert [25], who observed the complete degradation rate of a 50:50 mixture of poly-L-lactic acid and poly-D-lactic acid at 60 days in SBF. However, this accelerated degradation kinetics observed by Vert [25] was likely due to the polymer blend composition utilized.

According to Middleton and Tipton [11], the degradation rate depends on the amount of each homopolymer, L-lactide and D-lactide [11]. The degradation time of PLLA is much longer compared to PLDLA and required more than 2 years to take place in human [12]. In general, increasing the amount of D-lactide increases the material degradation kinetics due to the amount of amorphous polymer present in the copolymer. In our study, the mixture was 70:30 (poly-L-lactic acid and poly-D-lactic), and the degradation occurred in a slower fashion.

Compared to the degradation onsets observed in the present study (359.8–365.6°C), Chen et al. [26] found lower thermal onset degradation temperatures while characterizing biodegradable PLA polymeric blends (315.5–290.3°C). Our study analyzed 70/30 PLDLA in powder and pellet forms in the as-received and after different degradation times in SBF, while Chen et al. [26] evaluated the degradation as a function of the percentage of each lactide, from pure PLLA to pure PLDLA. The lower values observed by Chen et al. [21] could be explained by possible synthesis processes utilized in the different studies (a commercially available product was utilized in the present study—no information about processing conditions was provided by the manufacturer), since polymer micromorphologic characteristics are significantly affected by solidification rates (crystalline domain content), surface morphology, and material bulk structure.

A thermal stability decrease as a function of immersion time was observed for the pellet form, 365.6°C to 360.3°C, and for the powder form, 363.5°C to 359.8°C. This decrease likely occurred due to the PLDA homopolymers degradation that from a theoretical standpoint should occur earlier than the breakdown of PLLA homopolymers. After PLDA, which stability is lower than the PLLA one, be entirely degradated, the thermal stability decrease should occur more slowly as PLLA homopolymers is more stable than PLDA homopolymers. These results are in accordance to those obtained by Rezende et al. [27].

The endothermic peaks (Table 3) of approximately 124.5°C and 120°C related to the melting points were obtained for PLDLA in the pellet and powder forms, respectively. Despite the average difference between forms, these results were not significantly different ($P > 0.05$). The glass transition temperature was approximately 61.5°C and 64.6°C for the pellet and powder material, respectively. No significant differences ($P > 0.05$) in T_g was observed as a function of immersion time for the pellet material. However, significant variations in T_g as a function of immersion time was observed for the powder form. Between pellet and powder samples, T_g was significantly different after 30, 60, and 90 days of immersion in SBF (Table 3).

According to Daniels et al. [28] PLLA melting point is of 175–178°C and glass transition temperature of 60–65°C and to Bergsma et al. [29] the melting temperature of PLLA is about 174–184°C and the glass transition temperature of 57°C. Ferreira et al. [30] defined glass transition temperature of PLLA being 54°C and the melting temperature of 178°C. The glass transition temperature obtained in our study agrees to those described in the literature, but the results described in the literature for the melting temperature were higher than those obtained in our study. However, it should be noted that different compositions and processing routes were utilized in different studies.

The specific heat (c) was approximately 8.5 J/g and 6.2 J/g for the pellet and powder material, respectively. No significant difference in c was observed as a function of immersion time for the pellet and the powder. However, significant variations in c as a function of the milling process were observed between both materials (Table 3). Polymers with lower specific heat are more crystalline than those with higher specific heat. Thus the material in the powder form presented higher crystalline content than that in the pellet form. As previously indicated in the literature, the milling process may have resulted in the disruption of the large initial polymeric chains into smaller chains that increased the polymer crystalline content due to their rearrangement following disruption [27]. Further studies considering specific characterization tools for crystalline

content investigation as a function of in vitro immersion in different solutions are recommended.

5 Conclusion

Synthetic grafting materials have been utilized in clinical practice in a variety of forms, including bioceramics, polymeric, and combination of different materials. Polymer blends have been utilized in the past as bone filling and fracture fixation devices due to one's ability to tailor its mechanical and physical chemical properties. Our study investigated the effect of cryogenic milling on the degradation and physical properties of PLDLA pellets before and after immersion in SBF. According to the results obtained, cryogenic milling resulted in particle surface plastic deformation, and alterations in glass transition temperature, melting temperature, and specific heat of the starting material, suggesting that similar behavior is expected for both forms in vivo. Since grafting materials properties such as particle size and distribution and packability may play significant roles on the host-to-grafted region response, in vivo evaluation in a suitable craniofacial model should be topic of future research.

Acknowledgments Thanks to Prof. Sidnei Paciornik, Image Digital Processing Laboratory, PUC-Rio, Rio de Janeiro, Brazil for processing the images and supplying the data for particle size distribution analysis, and to Major Cano, Department of Chemical Engineering, Military Institute of Engineering, Rio de Janeiro, Brazil for helping with the Thermal Analysis. This research was financially supported by CNPq (Brazil) grant 300216/94–7, 452834/03-1, 50016/052003 and 472449/2004-4, FAPERJ (Brazil) grant E-26/151.970/2004 and CAPES (Brazil). This research was also partly supported by the Department of Biomaterials and Biomimetics, New York University, College of Dentistry.

References

1. C. Chaput, A. Selmani, C.H. Rivard, Curr. Opin. Orthop. **7**, 62–68 (1996)
2. J. Hench, J. Wilson, *An Introduction to Bioceramics. Advanced Series in Ceramics* (World Scientific Publishing Co. Pte. Ltd, Singapore, 1993), p. 386
3. B.N. Summers, S.M. Eisenstein, J. Bone. Joint. Surg. Br. **71**, 677–680 (1989)
4. A. Gadzag, J.M. Lane, D. Glaser, R.A. Forster, J. Am. Acad. Orthop. Surg. **3**, 1–8 (1995)
5. J. Devin, M. Attawia, C.T. Laurencin, J. Biomed. Sci. **7**,661–669 (1996)
6. T. Furukawa, Y. Matsusue, T. Yasunaga, Y. Nakagawa, Y. Okada, Y. Shikinami, M. Okuno, T. Nakamura, J. Biomed. Mater. Res. **50**, 410–419 (2000)
7. R. Suuronen, T. Pohjonen, J. Hietanen, C. Lindqvist, J. Oral. Maxillofac. Surg. **56**, 604–614 (1998)
8. P.A. Gunatillake, R. Adhikari, Eur. Cell. Mater. **5**, 1–16 (2003)
9. M. Borden, S.F. El-Amin, M. Attawia, C.T. Laurencin, Biomaterials **24**, 597–609 (2003)
10. S. Aslan, L. Calandrelli, P. Laurienzo, M. Malinconico, C. Migliaresi, J. Mater. Sci. **35**, 1615–1622 (2000)
11. J.C. Middleton, A.J. Tipton, Biomaterials **21**, 2335–2346 (2000)
12. J. Bergsma, W.C. De Bruijn, F.R. Rozema, R.R.M. Bos, G. Boering, Biomaterials **16**, 25–31 (1995)
13. D.K. Gilding, A.M. Reed, Polymer **20**, 1459–1464 (1979)
14. P. Rokkanen, O. Bostman, S. Vainionpaa, K. Vihtonen, P. Tormala, J. Laiho, J. Kilpikari, M. Tamminmaki, Lancet **1**, 1422–1424 (1985)
15. M. Kamogawa, A.R.A. Nogueira, L.M. Costa, E.E. Garcia, J.A. Nóbrega, Spectrochim. Acta Part B **56**, 1973–1980 (2001)
16. S. Gouveia, G.S. Lopes, O. Fatibello-Filho, A.R.A. Nogueira, J.A. Nóbrega, J. Food. Eng. **51**, 59–63 (2002)
17. J. De Boer, F.J.M.J. Maessen, Anal. Chim. Acta **177**, 371–375 (1980)
18. D. Koglin, F. Backhaus, J.D. Schladot, Chemosphere **34**, 2041–2047 (1997)
19. M. Wilczek, J. Bertling, D. Hintemann, Int. J. Min. Proces. **74S**, S425–S434 (2004)
20. D. Santos Jr., A.C. Tomazelli, F.J. Krug, J.A. Nóbrega, VI Workshop sobre Preparo de Amostras 57–68 (2006)
21. T. Kokubo, H. Takadama, Biomaterials **27**, 2907–2915 (2006)
22. S. Paciornik, M.H.P. Mauricio, in *Digital Imaging*, ed. by G. Vander Voort. ASM Handbook—Metallography and Microstructures (ASM International, Materials Park, 2004), pp. 368–402
23. C. Landes, A. Ballon, C. Roth, J. Biomed. Mater. Res. Part B Appl. Biomater. **76B**, 403–411 (2006)
24. A. Ribeiro, C.N. Elias, M.T.S. Araújo, J.S. Saloman, Revista Brasileira de Implantodontia **11**, 8–12 (2005)
25. M. Vert, P. Christel, F. Chabot, F.J. Leray, in *Bioresorbable Plastic Materials for Bone Surgery*, ed. by G. Hasting, P. Ducheyne. Macromolecular Biomaterials (CRC Press, Boca Raton, FL, 1984), pp. 120–142
26. C.C. Chen, J.Y. Chueh, H. Tseng, H.M. Huang, S.Y. Lee, Biomaterials **24**, 1167–1173 (2003)
27. C. Rezende, E.A.R. Duek, Polímeros Ciência e Tecnologia **13**, 36–44 (2003)
28. A.U. Daniels, M.K. Chang, K.P. Andriano, J. Appl. Biomater. **1**, 57–78 (1990)
29. E. Bergsma, F.R. Rozema, R.R.M. Bos, W.C. De Bruijn, J. Oral. Maxillofac. Surg. **51**, 666–670 (1993)
30. B. Ferreira, C.A.C. Zavaglia, E.A.R. Duek, Revista Brasileira de Engenharia Biomédica **19**, 21–27 (2003)